Progress In Electromagnetics Research B, Vol. 51, 101–118, 2013

DIFFERENTIAL EVOLUTION ALGORITHM FOR OPTIMIZING THE CONFLICTING PARAMETERS IN TIME-MODULATED LINEAR ARRAY ANTENNAS

S. K. Mandal*, **G. K. Mahanti, and Rowdra Ghatak**

Microwave and Antenna Research Laboratory, Department of Electronics and Communication Engineering, National Institute of Technology, Durgapur, West Bengal, India

Abstract—In this paper, a new technique is proposed to optimize the conflicting parameters like low value of maximum side lobe level (SLL), narrow beam-width of the main beam and low value of maximum sideband radiation level (SRL) of time-modulated linear antenna arrays (TMLAAs). The method is based on minimizing a multi-objective fitness function by using single-objective differential evolution algorithm (DEA) technique. The method is applied to both uniformly excited TMLAA (UE-TMLAA) and non-uniformly excited TMLAA (NUE-TMLAA) to synthesize low side lobe optimum pattern at operating frequency by suppressing the sideband radiation level to a sufficiently low value. For UE-TMLAA only the switch-on time durations of the array elements and for NUE-TMLAA the switch-on time durations and the static amplitudes with predetermined dynamic range ratio (DRR) of static amplitudes are taken as the optimization parameters for the DEA. To show effectiveness of the proposed approach, the single-objective DEA optimized results are compared with those obtained by other single objective and multi-objective techniques that has been reported previously. Also, first null beam width (FNBW) and half power beam width (HPBW) of the DEA optimized patterns at fundamental radiation are compared with those of the Dolph-Chebyshev (D-C) pattern of same SLL.

Received 27 February 2013, Accepted 11 April 2013, Scheduled 18 April 2013
* Corresponding author: S. K. Mandal (skmandal2006@yahoo.co.in).

1. INTRODUCTION

In 1959, Shanks and Bickmore commenced the theory of time modulation technique to control the radiation characteristics of antenna array [1] by introducing an additional degree of freedom 'time' as an antenna design parameter. Kummer et al. in 1963 first utilized the technique to realize the power pattern of ultra low SLL (∼39 dB) from a uniformly excited eight element slot linear antenna array [2]. The main advantage of the technique is that simple high speed switching circuits connected to each array elements are used to tapper the aperture excitations by periodically controlling the 'ON' time duration of the switches. Electronically, the relative on-time durations of the switches can be organized easily, rapidly, and accurately in a predetermined time sequence. Thus, the technique greatly reduces the design complexity of the array feeding network for achieving low side lobe pattern by relaxing the stringent requirement of the static amplitude distribution of the array elements. However due to periodical switching of the time modulated elements, in addition to the operating frequency TMLAA also radiates signal at different harmonics of the switching frequency, called side band radiation (SBR) [3]. In some applications, it is desired to minimize the sideband radiation level (SRL) as it reduces the radiation efficiency at the operating frequency and the directivity of the antenna array [4]. In order to increase the gain of the antenna array, in 2002 Yang and Qing [5] minimized simultaneously the side lobe level and SRL by using an optimization method based on differential evolution algorithm (DEA). Basically, TMLA synthesis problems are multi-objective optimization problems where the multiple objectives are low SLL and narrow beam width (BW) of the main beam at operating frequency and low SRL. After Yang, many other researchers have been attracted to this subject and during the past decade including DEA [6–8] different other evolutionary algorithms like genetic algorithm (GA) [9], simulated annealing (SA) [10, 11], artificial bee colony (ABC) algorithm [12], particle swarm optimization (PSO) [13, 14], multi-objective evolutionary algorithm based on objective decomposition with differential evolution operator (MOEA/D-DE) [15] have been applied to synthesize the desired pattern at the operating frequency by reducing the side band radiation level. In [6], the time modulation technique is applied to synthesize flat top power pattern in TMLAA with low DRR of static amplitude distribution. An array thinning procedure in NUE-TMLAAs is introduced in [7]. Without phase shifters, a beam steering technique at sidebands of TMLAAs is presented in [8] and also DEA is employed to improve the gain of the array. In [9], a UE-TMLAA with low SLL and SRL is designed by optimizing the 'on-time' sequences of the array elements and in [10, 12] the 'on-time' duration of the array elements are optimized to suppress both SLL and SRL. In [11], sum and difference patterns are synthesized by time modulating a small number of elements in linear antenna array. A pulse shifting method for synthesizing array patterns is proposed in [13]. The time dependent performance of TMLAAs is presented in [14]. In [15], MOEA/D-DE is applied to improve the conflicting specification of TMAAs. In [16], a closed form relationship between the power losses due to sideband radiation and the modulation sequence is used to minimize the power losses in time modulated arrays by constraining the radiation pattern at the carrier frequency below fixed side lobe level. The techniques for reducing the power losses of directive TMLAAs and time modulated planar arrays are suitably addressed in [17–19] respectively. Also a hardware based method in [20] and in [21] a modified switching circuit in combined with the limited bandwidth of the practical radiating elements have been exploited to suppress the side band power. Recently in [22], the DEA is applied to optimize the sub-sectional time steps for designing a low side lobe TMLAA with uniform amplitude. DEA is an efficient stochastic evolutionary computational algorithm and has been applied to solve many problems in different area such as, inverse scattering [23], antenna arrays [6–8, 24], engineering [25] and electromagnetics [26].

In [5–16, 22], different techniques based on different optimization tools are applied to optimize TMLAAs by suppressing the SLL and SRL to sufficiently low value. However, the optimized patterns at the carrier frequency is obtained either by constraining the FNBW to a predetermined value or without considering it. As a result, although the synthesized patterns at the carrier frequency are obtained by suppressing sideband level, the resultant patterns at the carrier frequency is not an optimum pattern, i.e., the synthesized pattern is not of minimum beam width for a specified side lobe level. Hence, the beam width of the fundamental pattern can be improved further. In this paper, DEA [23–26] is applied to obtain the lowest value of the FNBW for the power pattern at operating frequency by simultaneously reducing the SLL and SRL to predetermined values. The approach based on the minimization of the multi-objective fitness function by using single objective DEA technique synthesizes low side lobe narrow beam patterns at operating frequency of TMLAAs with reduced SRL. It is observed that the synthesized patterns at the operating frequency are closed to the Dolph-Chebyshev pattern.

2. THEORETICAL BACKGROUND OF TIME MODULATED LINEAR ARRAY

We consider a linear broadside array of N number of mutually uncoupled isotropic radiators with inter-element spacing d_0. All the radiators are excited by a sinusoidal signal of frequency $\omega_0 = 2\pi f_0$ and the radiating elements are on periodically in a predetermined on-time sequence t_p^{on} $(0 \leq t_p^{on} \leq T_m)$ $\forall p \in [1, N]$, in each time period, T_m. The periodical excitation of the array elements leads to decompose the array factor by applying Fourier series technique and the resulting array factor expression at k-th harmonics can be written as in Eq. (1) [3, 8].

$$AF_k(\theta, t) = e^{j(\omega_0 + k\omega_m)t} \sum_{p=1}^{N} A_p \tau_p \frac{\sin(k\pi\tau_p)}{k\pi\tau_p} e^{-j[k\pi\tau_p - (p-1)\beta d_0 \cos\theta]} \quad (1)$$

where $\omega_m = 2\pi/T_m = 2\pi f_m$ is the modulation frequency; A_p and $\tau_p = t_p^{on}/T_m$ $\forall p \in [1, N]$ stand for the normalized static amplitudes and on-time durations of the array elements respectively. From (1) it is seen that the array factor expression of the fundamental component $(k = 0)$, AF_0 provides the radiation pattern at the operating frequency. Although the equivalent τ_p's $\forall p \in [1, N]$ for UE-TMLAA [2] or the dynamic excitation distributions, $E_p = A_p \tau_p$ $\forall p \in [1, N]$ with predetermined DRR for NUE-TMLAA [5] can be obtained directly by using Dolph-Chebyshev method to produce the optimum pattern of specific SLL and beam width at the operating frequency. But the method cannot control the sideband radiation. Moreover, to what extent a trade-off between the SLL and SRL can be realized for a TMLAA that is unknown. In this paper, the authors try to get the solutions of such problems by employing single objective DEA technique.

3. DIFFERENTIAL EVOLUTION ALGORITHM (DEA)

The block diagram of DEA used to optimize the TMLA synthesizing problems is explained in Fig. 1. The two main stages of the algorithm are initialization and evolution. At initialization, the optimization process is started by the initial population G^0, consisting of S number of D dimensional parameter vectors, $\vec{V}_s^0 = \{v_{z,s}^0\}$, $s = 1, 2, \ldots, S$ and $z = 1, 2, \ldots, D$. The superscript in a parameter represents the generation index of the parameter, e.g., G^g is the population at generation 'g'. The parameter vectors in G^0 are randomly generated within the search space bounded by the lower limits (i.e., $\vec{V}_{\min} = v_{z,\min}$, $z = 1, 2, \ldots, D$) and upper limits (i.e., $\vec{V}_{\max} = v_{z,\max}$, $z =$

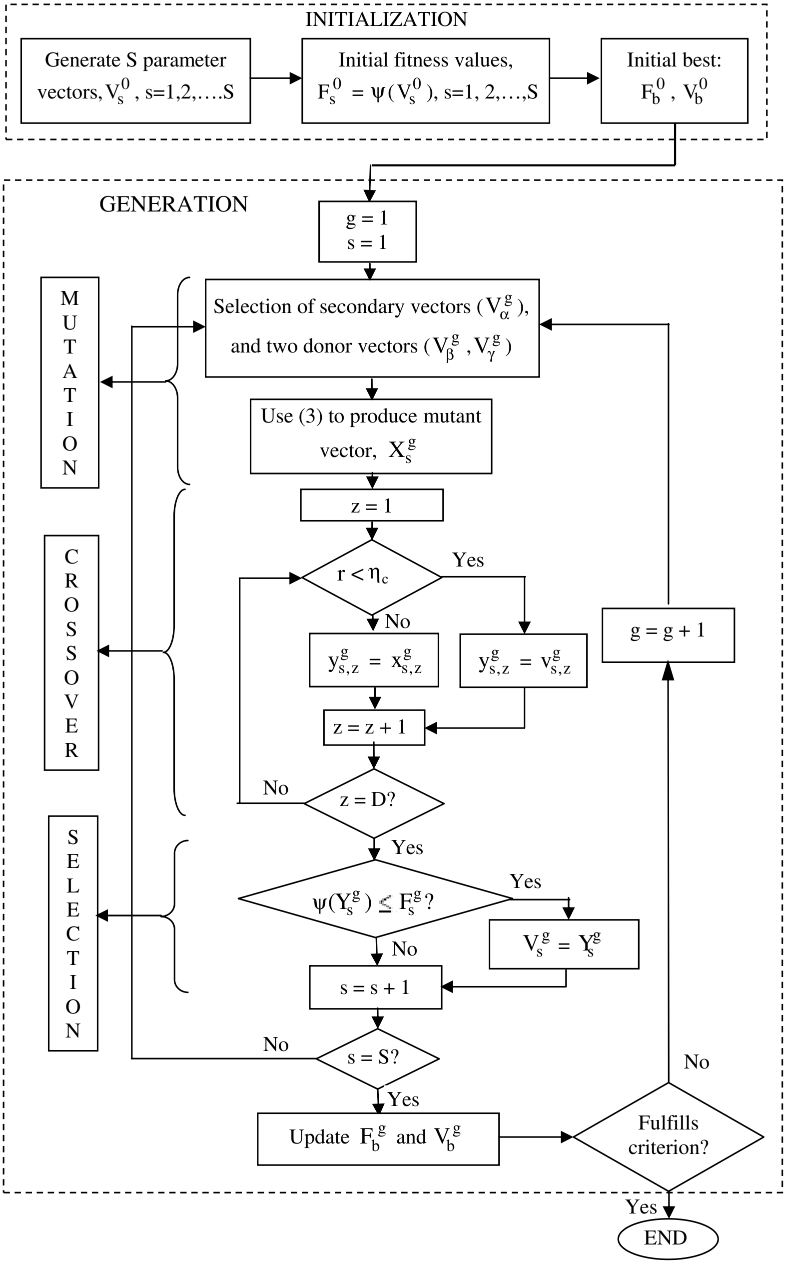

Figure 1. The block diagram of DEA with DE/rand/1/bin strategy.

1, 2, ..., D) of the parameter values. In the sth vector, the value of zth parameter is obtained as

$$v^0_{z,s} = v^{\min}_z + \text{rand}_{z,s}(0,1) \cdot \left(v^{\max}_z - v^{\min}_z\right) \tag{2}$$

where $\text{rand}_{z,s}(0,1)$ is a stochastic variable uniformly distributed between 0 and 1, i.e., $0 \le \text{rand}_{z,s}(0,1) \le 1$. Now, corresponding to the each individuals of G^0, the values of the fitness function ψ, i.e., $F^0_s = \psi(\vec{V}^0_s)$, $s = 1, 2, \ldots, S$ and their best values, F^0_b, $\vec{V}^0_b$ are set. F^0_b is the minimum value of the fitness function for the parameter vector $\vec{V}^0_b$.

Like genetic algorithm (GA), the next stage of DEA is evolution. In evolution, iteratively three genetic operators, mutation, crossover and selection are executed sequentially to generate the new vectors for the next generation. However, in DEA the execution sequence of the operators is first mutation, then crossover and finally selection, whereas in GA generally the execution order is crossover, selection and mutation. In DEA, the operators are implemented as follows.

With respect to GA, the main difference in DEA is mutation. Biologically, the abrupt change in the gene characteristics of a chromosome is known as 'mutation'. In the model of evolutionary computing, each individual (i.e., $\vec{V}^g_s$, $s = 1, 2, \ldots, S$) of the current population is identified as chromosome. For a given optimization problem, the real coded parameter values (i.e., $v^g_{z,s}$, $z = 1, 2, \ldots, D$) to be optimized are the gene of the chromosome $\vec{V}^g_s$. To realize mutation operation in DEA, corresponding to each primary parent vectors $\vec{V}^g_s$, $s = 1, 2, \ldots, S$, of the current generation 'g', a mutant vector ($\vec{X}^g_s = \{x^g_{z,s}\}$) is produced. To form a mutant vector, a secondary vector, $\vec{V}^g_\alpha = \{v^g_{z,\alpha}\}$, $z = 1, 2, \ldots, D$ is perturbed by adding the weighted difference of two donor vectors, $\vec{V}^g_\beta = \{v^g_{z,\beta}\}$, $z = 1, 2, \ldots, D$ and $\vec{V}^g_\gamma = \{v^g_{z,\gamma}\}$, $z = 1, 2, \ldots, D$, as given in (3).

$$\vec{X}^g_s = \vec{V}^g_\alpha + F \cdot \left(\vec{V}^g_\beta - \vec{V}^g_\gamma\right) \tag{3}$$

where the vector indexes α, β and γ are mutually exclusive to each other and randomly chosen from the range [1, S] such that these are different from the primary vector index 's'. F is a scalar number, known as mutation constant and its typical value lies between [0.4, 1].

The binomial crossover method is applied to enhance the potential diversity of the population. In crossover operation, new children vectors $\vec{Y}^g_s = \{y^g_{z,s}\}$ are formed by exchanging the components of the parent vectors and the mutant vectors. The components of the children vector are obtained as follows

$$y_{z,s}^{g} = \begin{cases} v_{z,s}^{g} & \text{if } (\text{rand}_{z,s}(0,1) \le \eta_c \text{ or } z = z_{\text{rand}}) \\ x_{z,s}^{g} & \text{otherwise} \end{cases} \quad (4)$$

where, $\text{rand}_{z,s}(0,1)$ is a randomly generated number between (0, 1) and the randomly chosen index, $z_{\text{rand}} \in [1, 2, \ldots, D]$ ensures that $\vec{Y}_s^g$ must have at least one component from $\vec{V}_s^g$. The parameter $\eta_c \in (0,1)$ is known as crossover constant.

Thus, children vectors are obtained by executing the two operators, mutation and crossover. In the mutation scheme, the secondary vector $\vec{V}_\alpha^g$ is selected randomly and the vector is perturbed by adding one scaled difference vector $F \cdot (\vec{V}_\beta^g - \vec{V}_\gamma^g)$. The corresponding mutation scheme is expressed as DE/rand/1. When the mutation scheme is combined with the crossover method, which is currently binomial, the notation of the DEA strategy becomes DE/rand/1/bin. More details about the DEA and DEA strategies can be found in [19–21].

The selection operator is used to keep the population size constant at each consecutive generation of the optimization process. In this operation, either target vector, i.e., the parent vector of the current generation ($\vec{V}_s^g$) or the trial vector, i.e., the corresponding children vector ($\vec{Y}_s^g$) is selected as the parent vector for the next generation. The selection mechanism is

$$\begin{aligned} \vec{V}_s^{g+1} &= \vec{Y}_s^g \text{ if } \psi\left(\vec{Y}_s^g\right) \le \psi\left(\vec{V}_s^g\right) \\ &= \vec{V}_s^g \text{ if } \psi\left(\vec{Y}_s^g\right) > \psi\left(\vec{V}_s^g\right) \end{aligned} \quad (5)$$

Now the new population vectors are ready for the next generation. For the current population G^g, if the new best value of the fitness function F_b^g outperforms the old best, the best value and the corresponding vector (i.e., $\vec{V}_b^g$) is updated and the evolution process of the population is repeated till the termination criterion is fulfilled. A predetermined value of the fitness function or maximum number of generation '$g_{\max}$' is used as the termination criterion of the optimization process. The optimization process may not always provide the desired value of the fitness function. Under this situation, the optimum solution of the optimization problem is that vector of the last population for which the fitness function value is the lowest.

4. THE FITNESS FUNCTION FOR OPTIMIZATION OF TMLAA

To optimize the conflicting parameters, i.e., SLL, SRL and FNBW in TMLAA, the fitness function is defined as

$$\psi^g(\vec{V}_s^g) = \sum_{i=0}^{i=2} W_i \cdot \mathrm{H}(\Delta_i) \cdot \Delta_i^2 + W_3 \cdot FNBW^g(\vec{V}_s^g) \tag{6}$$

with $\Delta_0(\vec{V}_s^g) = |SLL_d - SLL_{\max}^g(\vec{V}_s^g)|$, $\Delta_1(\vec{V}_s^g) = |SRL_{1,d} - SRL_1^g(\vec{V}_s^g)|$, $\Delta_2(\vec{V}_s^g) = |SRL_{2,d} - SRL_2^g(\vec{V}_s^g)|$. In (6), SLL_d, $SRL_{1,d}$, $SRL_{2,d}$ are the desired values of the maximum SLL at the fundamental frequency and maximum SRL at the first and second harmonics respectively and FNBW is the obtained value of first null beam-width to be minimized. $SLL_{\max}^g$ is the calculated maximum SLL at generation 'g' when the optimization parameter vector is $\vec{V}_s^g$. For UE-TMLAA, $\vec{V}_s^g$ is defined as $\vec{V}_s^g = \{\tau_p, \forall p \in [1, N]\}$ while for NUE-TMLAA, it becomes $\vec{V}_s^g = \{\tau_p, A_p \colon \forall p \in [1, N]\}$. SRL_1^g and SRL_2^g are the corresponding maximum values of sideband level obtained at first and second sideband respectively. $H(\cdot)$ is the Heaviside step function. W_0, W_1, W_2 and W_3 are the weighting factors of the corresponding terms. The values of the weighting factors are assigned based on the priority order of the corresponding objectives. The primary objective is to minimize FNBW by suppressing SLL and SRLs to the desired predetermined values. But, the large value of W_3, i.e., weighting factor corresponding to FNBW may not give the optimal solution by selecting low value of FNBW of relatively high side lobe pattern. Since during the optimization process, when the first three objective values are approaching to their desired values, the corresponding differences Δ_i, $i = 0$, 1 and 2 are iteratively reduced to infinitesimally small values. Moreover from (1), it is observed that due to the p-th element, the radiation at k-th harmonics ($k \neq 0$) is proportional to $[A_p \frac{\sin(k\pi\tau_p)}{k\pi}]$. As a result, significance to suppress the first sideband is more than the second sideband. Hence, the priority orders of the four objectives of (6) are set as: first SLL, second SRL at first sideband, third FNBW and after that SRL at second sideband. In the following examples in Section 5, at first the weighting factors are chosen in the following way,

i) $W_0 \geq W_1 \geq W_3 > W_2$
ii) $W_1 : W_2 \approx 2 : 1$.

However, the final values of the weighting factors obtained by trial and error are given in the corresponding examples.

5. NUMERICAL RESULTS AND COMPARISONS

To show the effectiveness of the proposed approach, the following four examples are considered for a 30 element TMLAA. The array is assumed to lie on the positive side of the Z-axis with one element at the origin. In the first example, let us assume that the array is uniformly excited TMLAA (UE-TMLAA) with inter-element spacing, $d_0 = 0.7\lambda$ (λ being the operating wavelength). For uniform excitation of static amplitudes ($A_p = 1$, $\forall p \in [1, N = 30]$), only the normalized on-time durations τ_p, $\forall p \in [1, N]$ are taken as the optimization parameters for the DEA. Thus, the optimization parameter vector $\vec{V}^g = \{\tau_p\}$, $\forall p \in [1, N]$ is used to reduce the fitness function in (6). To compare the DEA optimized results with that obtained by using SA [10] and MOEA/D-DE [15], the search range for the normalized on-time duration is chosen as $\tau_p \in [0.06, 1]$, $\forall p \in [1, N]$ which is same as considered in [10, 15]. With the desired values of SLL at the operating frequency, $SLL_d = -20.6$ dB and the sideband radiation levels (SRLs) in the first two sidebands, $SRL_{1,d} = -30$ dB and $SRL_{2,d} = -30$ dB respectively, DEA determines the optimum value of the FNBW of the main beam pattern at the operating frequency after 500 iteration. In (6), the values of weighting factors are selected as 25, 22, 11 and 1.5, respectively. The DEA optimized pattern is shown in Fig. 2, and the corresponding on-time durations of the array elements are given in Table 1. The performance of DEA optimized result and those obtained in [10, 15] are compared in Table 2, Example-I. In Table 2, the method 'D-C to UE-TMLAA' represents the direct application of the Dolph-Chebyshev (D-C) method to UE-TMLAA where the numerical values of the on-time durations are made equal to the normalized static amplitude distribution of the Dolph-Chebyshev pattern of same SLL as obtained by DEA. Since the D-C method gives the optimum pattern, i.e., the pattern with minimum BW for a specific value of SLL or, vice versa; at fundamental radiation of TMLAA. But, in this method the undesired SRL is high. Since the performance of MOEA/D-DE [15] is better than that optimized by SA [10]. Now, comparing the DEA optimized results to that of MOEA/D-DE, it can be observed that with almost same value of maximum SRL, the maximum SLL and FNBW of the DEA optimized pattern are 0.2 dB and 0.3° less than that obtained by MOEA/D-DE. To see the DEA optimized pattern's closeness to the optimum pattern, the beam widths (BWs), i.e., FNBW and HPBW of the main beam of fundamental pattern are compared with that of the Dolph-Chebyshev (D-C) pattern of same SLL. From Table 2 it can be seen that FNBW and HPBW of the DEA optimized pattern are only 0.52° and 0.14° higher than that of the D-C pattern.

In the second example, the array is assumed symmetrical NUE-TMLAA. As the array is symmetrical, only half of the number of optimization parameters is needed. To minimize the fitness function as expressed in (6), DEA directly optimizes the parameter vector $\vec{V}^g = \{\tau_p, A_p\}$, $\forall p \in [1, N/2]$, with the search space for A_p and τ_p as (0.5, 1) and (0.197, 1), respectively. The desired values of SLL and SRLs are set to -30 dB and W_i's ($i = 0, 1, 2, 3$) are chosen as 11, 7, 3 and 5, respectively. The DEA optimized far-field radiation pattern is shown in Fig. 3(a), and the optimum normalized amplitude distribution and switch-on time duration are shown in Fig. 3(b). In Fig. 3(a), the SLL and FNBW of the fundamental pattern are obtained as -29.44 dB and 7.98°, respectively. As can be seen from Example-2 of Table 2, as compared to [7] the proposed method improves the SLL, FNBW and HPBW by 6.43 dB, 4,75° and 1.3°, respectively, with 4 dB higher value of SRL (-30.02 dB). The improvement in BW is expected, as the synthesized pattern in [7] is obtained by discarding few (seven) array elements. However the simultaneous reduction in both SLL and BW proves the better optimizing performance of the proposed approach. Example 2 in Table 2 shows that with respect to the D-C pattern of same SLL, the FNBW and HPBW of the DEA optimized pattern are only 0.14° and 0.02° higher respectively.

In the third example, DEA is applied to optimize two antenna arrays with number of element 30 and 32. First, a 30 element antenna array of inter element spacing, $d_0 = 0.5\lambda$ is considered so as to compare the DEA optimized result of this example with that obtained in [5, 15].

The static amplitudes and normalized switch-on time durations are perturbed in the search range of $A_p \in (0.25, 1)$ and $\tau_p = (0.07, 1)$ respectively so that with low DRR (= 4) of static amplitudes and

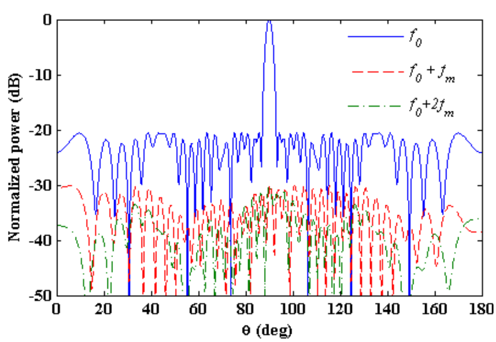

Figure 2. DEA optimized radiation pattern of fundamental (f_0) and first two sidebands ($f_0 + f_m$, $f_0 + 2f_m$) of UE-TMLA.

Table 1. Element wise normalized on-time durations, $\tau_p \, \forall \, p \in [1, N = 30]$ of the DEA optimized pattern shown in Fig. 2.

Element Number	Normalized on-time duration, τ_p
1	0.991
2	0.630
3	0.109
4	0.989
5	0.988
6	0.959
7	0.891
8	0.947
9	1.0
10	1.0
11	0.999
12	1.0
13	1.0
14	1.0
15	1.0
16	1.0
17	1.0
18	1.0
19	1.0
20	1.0
21	0.941
22	0.965
23	0.948
24	0.866
25	0.0663
26	0.204
27	0.105
28	0.877
29	0.133
30	0.993

sufficiently high value of the switch-on time duration, the feed network of the array can be realized easily. The SLL_d, $SRL_{1,d}$ and $SRL_{2,d}$ are set to -58.5 dB, -30 dB and -30 dB respectively. The optimization parameter vector in this example is the same as that considered in

Table 2. Comparison of radiation parameters obtained by DEA with those obtained by other methods.

Examples	Methods	*SLL* (dB)	*FNBW* (Deg)	*HPBW* (Deg)	SRL_1 (deg)	SRL_2 (Deg)	DRR
I	**DEA**	**−20.60**	**6.7**	**2.7**	**−30.0**	**−30.0**	**1**
	D-C to UE-TMLAA	−20.6	6.18	2.56	−8.2	−16.96	1
	MOEA/D-DE [15]	−20.4	7.0	2.9	−30.1	-	1
	SA (Table 1, Ref. [7])	−20.0	9.34	3.84	−30.0	-	1
II	**DEA**	**−29.44**	**7.98**	**3**	**−30.02**	**−30.69**	**2**
	D-C to UE-TMLAA	−29.44	7.84	2.96	−12.29	−19.67	1
	Ref. [7]	−23.01	12.59	4.26	−34.08	-	2.04
III-A	**DEA**	**−58.5**	**19.12**	**5.62**	**−30.19**	**−33.62**	**4**
	D-C to UE-TMLAA	−58.5	18.98	5.6	−12.53	−17.35	1
	Ref. [5]	−50.0	20	-	−32.2	-	3.97
	Ref. [15]	58.5	20	-	−32.2	-	3.97
III-B	**DEA**	**58.5**	**17.78**	**5.24**	**−30.04**	**−32.06**	**3.97**
	D-C to UE-TMLAA	58.5	17.76	5.24	−12.53	−17.34	1
IV	**DE**	**−70.1**	**22.72**	**6.18**	**−30.04**	**−33.36**	**4**
	D-C to UE-TMLAA	−70.1	22.2	6.06	−12.49	−17.26	1

Example II, but search space of the parameters is different. The weighting factors are chosen as 25, 11, 5 and 7 respectively. Now, DEA optimizes the fundamental pattern with SLL and FNBW of −58.52 dB and 19.12° by suppressing the maximum SRL of first two sidebands to −30.19 dB and 33.62 dB respectively. The optimized pattern is shown in Fig. 4(a), and the corresponding static amplitudes and on-time durations of the switches are presented in Fig. 4(b), respectively. In [15], it is shown that the MOEA/D-DE based optimization results outperform DEA based single objective technique [5]. Both of these results are given in Table 1, Example-III-A. Now comparing MOEA/D-DE optimized result with the DEA optimized result of this example, as can be observed that with same value of SLL, the FNBW is 0.88° less

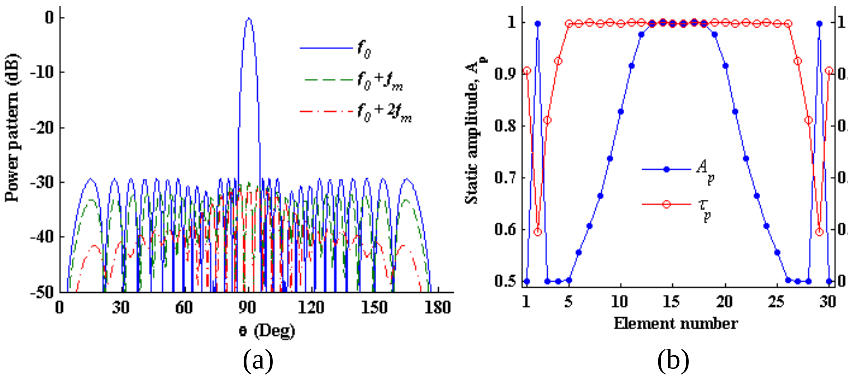

Figure 3. DEA optimized power pattern and the corresponding static amplitude and on-time duration for 30 elements TMLAA with DRR of static amplitude and on-time duration as in [5, 15]. (a) The normalized power pattern at fundamental radiation, f_0, and first two sidebands, $f_0 + f_m$ and $f_0 + 2f_m$. (b) Element wise distribution of normalized static amplitude and on-time duration of the array elements.

than that obtained by MOEA/D-DE [15]. It is noted in [5, 15] that the number of isotropic radiators in the antenna array is considered as 32 whereas the pattern in Fig. 4(a) is obtained by considering a 30 element TMLAA. Thus with lower number of radiating elements, the narrow beam pattern of the same SLL proves the better optimizing performance of the proposed approach. However, in this case, the maximum SRL (-30.2 dB) and DRR (4) are slightly higher than that in [5, 15] which are -32.2 dB and 3.97, respectively.

Now to realize the real optimization of the TMLA pattern over MOEA/D-DE, in the second case of this example, we consider all the constraints which can affect radiation pattern are same as considered in [15], i.e., the number of element in the array is 32 and the search space of τ_p and A_p are $\tau_p \in (0.06, 1)$ and $A_p \in (0.252, 1)$ respectively. The weighting factors are set to 30, 30, 16 and 2.5 respectively. The DEA optimized pattern of this example is shown in Fig. 5(a) and the corresponding radiation parameters are given in Example-III (B) of Table 2. The static amplitude distribution and the on-time duration of the pattern are shown in Fig. 5(b). As compared to MOEA/D-DE, the FNBW in DEA optimized pattern is improved by 2.22°. Moreover, the beam widths of the DEA optimized pattern are close to that of DC pattern of same SLL.

In the fourth example, search range for A_p is kept the same as that in Example-III (A), but the search range for τ_p's is chosen as $\tau_p = (0.02, 1)$. With the new search range of τ_p, we want to see whether

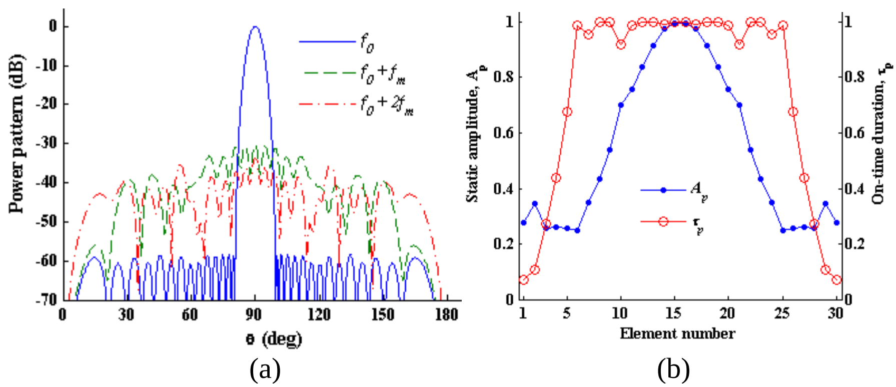

Figure 4. DEA optimized power pattern and the corresponding static amplitude and on-time duration for 30 elements TMLAA of Example III (A). (a) The normalized power pattern at fundamental radiation, f_0, and first two sidebands, f_0+f_m and f_0+2f_m. (b) Element wise distribution of normalized static amplitude and on-time duration of the array elements.

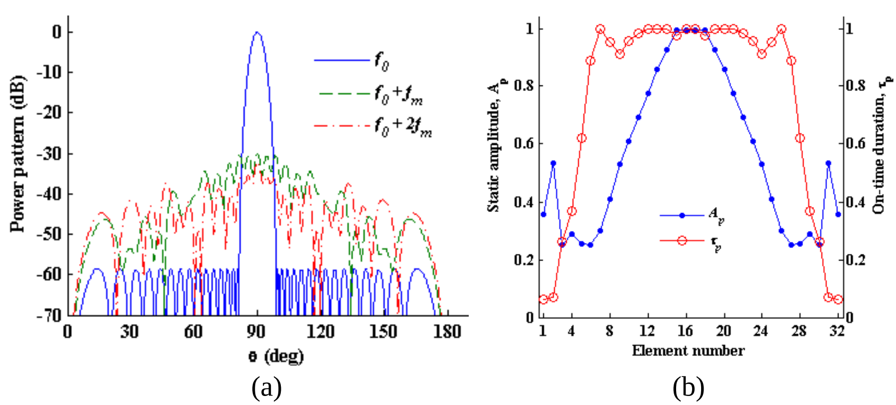

Figure 5. DEA optimized power pattern and the corresponding static amplitude and on-time durationfor 32 elements TMLAA with same search space of static amplitude and on-time duration as in [5] and [15]. (a) The normalized power pattern at fundamental radiation, f_0, and first two sidebands, $f_0 + f_m$ and $f_0 + 2f_m$. (b) Element wise distribution of normalized static amplitude and on-time duration of the array elements.

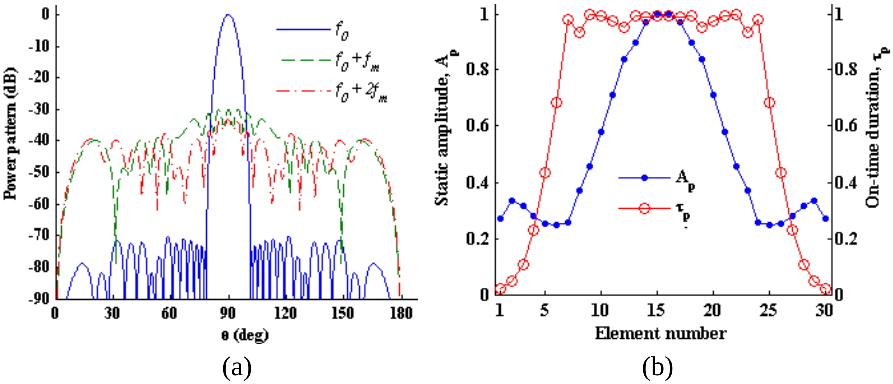

Figure 6. DEA optimized power pattern and the corresponding static amplitude and on-time duration for 30 elements TMLAA with the search space of static amplitude and on-time duration as prescribed in Example IV. (a) The normalized power pattern at fundamental radiation, f_0, and first two sidebands, f_0+f_m and f_0+2f_m. (b) Element wise distribution of normalized static amplitude and on-time duration of the array elements.

proposed method has the ability to reduce the SLL further. Now, the new value of SLL_d is set to -70 dB and W_i's ($i = 0, 1, 2$ and 3) are set to 300, 17, 8 and 2, respectively. Fig. 6(a) shows the DEA optimized pattern. Corresponding τ_p and A_p with $p = 1, 2, \ldots, N$ are shown in Fig. 6(b). As can be seen from Table 2, Example-IV, the beam widths (FNBW and HPBW) of the DEA optimized pattern are also comparable to that of the Dolph-Chebyshev pattern of the same SLL whereas the SRLs of the first two sidebands are suppressed to -30.04 dB and 33.36 dB, respectively.

6. CONCLUSIONS

Synthesis of time modulated antenna arrays is a multi-objective optimization problem. The main difficulty in such problems is to optimize the conflicting parameters like maximum SLL, FNBW and maximum SRL. In this paper, an approach based on single objective DEA is employed to optimize TMLAAs by determining the optimum value of the FNBW of the main beam power pattern by simultaneously reducing the SLL and SRL to a predetermined value. Compared to the previously reported results, the method synthesizes low side lobe narrow beam pattern with low value of SRLs. Also, the FNBW and half power beam width (HPBW) of the low side lobe DEA optimized fundamental patterns are in good agreement with that of the Dolph-Chebyshev pattern of the same SLLs. Thus, the approach can be used to optimize the conflicting parameters of TMLAAs.

REFERENCES

1. Shanks, H. E. and R. W. Bickmore, "Four dimensional electromagnetic radiators," *Canad. J. Phys.*, Vol. 37, No. 3, 263–275, 1959.
2. Kummer, W. H., A. T. Villeneuve, T. S. Fong, and F. G. Terrio, "Ultra-low side-lobes from time-modulated arrays," *IEEE Trans. Antennas Prop.*, Vol. 1, No. 6, 633–639, 1963.
3. Bregains, J. C., J. Fondevila-Gomez, G. Franceschetti, and F. Ares, "Signal radiation and power losses of time-modulated arrays," *IEEE Trans. Antennas Prop.*, Vol. 56, No. 6, 1799–1804, 2008.
4. Yang, S., Y. B. Gan, and P. K. Tan, "Evaluation of directivity and gain for time modulated linear antenna arrays," *Microw. Opt. Technol. Lett.*, Vol. 42, No. 2, 167–171, 2004.
5. Yang, S., Y. B. Gan, and A. Qing, "Sideband suppression in time-modulated linear arrays by the differential evolution algorithm," *IEEE Antennas Wireless Prop. Lett.*, Vol. 1, 173–175, 2002.
6. Yang, S., Y. B. Gan, and P. K. Tan, "A new technique for power-pattern synthesis in time-modulated linear arrays," *IEEE Antennas Wireless Propag. Lett.*, Vol. 2, 285–287, 2003.
7. Aksoy, E. and E. Afacan, "Thinned nonuniform amplitude time-modulated linear arrays," *IEEE Antennas and Wireless Prop. Lett.*, Vol. 9, 514–517, 2010.
8. Li, G., S. Yang, Y. Chen, and Z. Nie, "A novel electronic beam steering technique in time modulated antenna arrays," *Progress In Electromagnetics Research*, Vol. 97, 391–405, 2009.
9. Yang, S., Y. B. Gan, A. Qing, and P. K. Tan, "Design of uniform amplitude time modulated linear array with optimized time sequences," *IEEE Trans. Antennas and Prop.*, Vol. 53, No. 7, 2337–2339, 2005.
10. Fondevila, J., J. C. Bregains, F. Ares, and E. Moreno, "Optimizing uniformly excited linear arrays through time modulation," *IEEE Antennas Wireless Prop. Lett.*, Vol. 3, No. 1, 298–301, Dec. 2004.
11. Fondevila, J., J. C. Brégains, F. Ares, and E. Moreno, "Application of time-modulation in the synthesis of sum and

difference patterns by using linear arrays," *Microw. Opt. Technol. Lett.*, Vol. 48, 829–832, 2006.

12. Mandal, S. K., R. Ghatak, and G. K. Mahanti, "Minimization of side lobe level and side band radiation of a uniformly excited time modulated linear antenna array by using artificial bee colony algorithm," *Proceedings of IEEE Symposium on Industrial Electronics and Applications (ISIEA 2011)*, 247–250, Sep. 2011.
13. Poli, L., P. Rocca, L. Manica, and A. Massa, "Pattern synthesis in time-modulated linear arrays through pulse shifting," *IET Microw. Antennas Propag.*, Vol. 4, No. 9, 1157–1164, 2010.
14. Manica, L., P. Rocca, L. Poli, and A. Massa, "Almost time independent performance in time-modulated linear arrays," *IEEE Antennas Wireless Prop. Lett.*, Vol. 8, 843–846, 2009.
15. Chen, Y., S. Yang, and Z. Nie, "Improving conflicting specifications of time-modulated antenna arrays by using a multiobjective evolutionary algorithm," *Int. J. Numer. Model*, Vol. 25, No. 3, 205–215, Wiley Online Library, 2012.
16. Poli, L., P. Rocca, L. Manica, and A. Massa, "Handling sideband radiations in time-modulated arrays through particle swarm optimization," *IEEE Transactions on Antennas and Propagation*, Vol. 58, No. 4, 1408–1411, Apr. 2010.
17. Rocca, P., L. Poli, G. Oliveri, and A. Massa, "Synthesis of time-modulated planar arrays with controlled harmonic radiations," *Journal of Electromagnetic Waves and Applications*, Vol. 24, Nos. 5–6, 827–838, 2010.
18. Poli, L., P. Rocca, L. Manica, and A. Massa, "Time modulated planar arrays — Analysis and optimization of the sideband radiations," *IET Microw. Antennas Propag.*, Vol. 4, No. 9, 1165–1171, 2010.
19. Poli, L., P. Rocca, and A. Massa, "Sideband radiation reduction exploiting pattern multiplication in directive time-modulated linear arrays," *IET Microw. Antennas Propag.*, Vol. 6, No. 2, 214–222, 2012.
20. Tong, Y. and A. Tennant, "Reduced sideband levels in time-modulated arrays using half-power sub-arraying techniques," *IEEE Transactions on Antennas and Propagation*, Vol. 59, No. 1, 301–303, 2011.
21. Tong, Y. and A. Tennant, "Sideband level suppression in time modulated linear arrays using modified switching sequences and fixed bandwidth elements," *Electron. Lett.*, Vol. 48, No. 1, 10–11, 2012.

22. Zhu, Q., S. Yang, L. Zheng, and Z. Nie, "Design of a low side lobe time modulated linear array with uniform amplitude and sub-sectional optimized time steps," *IEEE Transactions on Antennas and Propagation*, Vol. 60, No. 9, 4436–4439, Sep. 2012.
23. Rocca, P., M. Benedetti, M. Donelli, D. Franceschini, and A. Massa, "Evolutionary optimization as applied to inverse scattering problems," *Inverse Problems, Topical Review*, Vol. 25, 1–41, Dec. 2009.
24. Lin, C., A. Qing, and Q. Feng, "Synthesis of unequally spaced antenna arrays by using differential evolution," *IEEE Transactions on Antennas and Propagation*, Vol. 58, No. 8, 2553–2561, Aug. 2010.
25. Das, S. and P. N. Suganthan, "Differential evolution: A survey of the state-of-the-art," *IEEE Trans. Evol. Comput.*, Vol. 15, No. 1, 4–31, 2011.
26. Rocca, P., G. Oliveri, and A. Massa, "Differential evolution as applied to electromagnetics," *IEEE Antennas Propag. Mag.*, Vol. 53, No. 1, 38–49, Feb. 2011.